THE ASTROPHYSICAL JOURNAL, 224:841–847, 1978 September 15

H_2 RESONANCE FLUORESCENCE WITH LYMAN-α

J. MICHAEL SHULL
Department of Physics and Astrophysics, University of Colorado; and
Joint Institute for Laboratory Astrophysics, University of Colorado and National Bureau of Standards
Received 1978 February 3; accepted 1978 March 23

ABSTRACT

Lyman-α radiation may excite Lyman-band fluorescence from vibrationally excited H_2. Because of the resonant nature of the process, pumping rates in various H_2 lines are dependent both on temperature and on the Lα profile. We compute absolute and relative pumping rates in the resonances, and describe the applications to the recently observed sunspot H_2 fluorescent emission and to interstellar gas.

Subject headings: interstellar: molecules — molecular processes — Sun: spectra

I. INTRODUCTION

Molecular hydrogen has been detected in the interstellar medium in both ultraviolet (UV) absorption (Carruthers 1970; Spitzer *et al.* 1973) and in infrared (IR) emission (Gautier *et al.* 1976; Grasdalen and Joyce 1976; Beckwith *et al.* 1977; Treffers *et al.* 1976). The IR and UV lines of H_2 also provide important diagnostics of the atmospheres of the major planets (Cochran, Gelfand, and Smith 1976).

Recently, approximately 100 emission lines between 1170 and 1700 Å in high-resolution rocket spectra of a sunspot were identified as belonging to the H_2 Lyman bands (Jordan *et al.* 1977). The observed lines originate from only a few upper levels in the excited $B\,^1\Sigma^+_u$ electronic state, evidently pumped from the $v'' = 2$ vibrational level of the ground $X\,^1\Sigma^+_g$ electronic state by resonance fluorescence with Lα. Of course, continuum UV is much more effective at pumping H_2, since there are many more lines available. But in many cases, such as the Sun, UV emission lines are several orders of magnitude more intense than the underlying continuum.

In this paper we examine this resonance fluorescence process in some detail. Because of the resonant nature of the excitation, the fluorescence rates depend on the Lα line profile and Doppler shift. Because the resonances require vibrationally excited H_2 ($v'' \geq 2$), the rates are also temperature-dependent. Hence in an optically thin situation, ratios of lines pumped from $v'' = 2$ and $v'' = 3$ provide temperature diagnostics, while ratios of lines pumped by resonances at varying distances from Lα line center provide profile diagnostics. In § II we describe the fluorescence process; in § III we present quantitative calculations of the LTE fluorescent pumping rates and line ratios, and in § IV we summarize the implications of this process for sunspots, the interstellar medium, and other objects.

II. LYMAN-BAND RESONANCES

The H_2 Lyman bands arise between the ground $X\,^1\Sigma^+_g$ electronic state and the excited $B\,^1\Sigma^+_g$ state, while the Werner bands connect to the excited electronic state $C\,^1\Pi_u$. Lyman and Werner absorption lines from the lowest ($v'' = 0$) vibrational level of $X\,^1\Sigma^+_g$ lie between approximately 850 and 1130 Å and 850 and 1020 Å, respectively. Consequently, resonant overlap with Lα (1215.670 Å) requires vibrationally excited H_2 ($v'' \geq 2$ for the Lyman bands and $v'' \geq 5$ for the Werner bands).

Radiative selection rules preclude Lα photodissociation of H_2 to the $X\,^1\Sigma^+_g$ vibrational continuum (4.477 eV), while photodissociation to the continua of the excited electronic states (14.675 eV) is ruled out energetically. Resonant H_2 line absorption of Lα will produce negligible dissociation ($< 10^{-8}$ per absorption) in cascade back to the vibrational continuum of $X\,^1\Sigma^+_g$ (Stephens and Dalgarno 1970).

The lines of H_2 which overlap Lα may be determined from the spectroscopic data of Fink, Wiggins, and Rank (1965), Herzberg and Howe (1959), and Herzberg (1950), combined with the tabulation of Lyman and Werner absorption lines from $v'' = 0$ by Morton and Dinerstein (1976). Table 1 lists the closest resonances in the Lyman bands of H_2 originating in $v'' = 2$ and $v'' = 3$, together with their oscillator strengths and excitation temperatures. For convenience in visualizing the relative pumping effectiveness of these resonances, we have shown them superposed on a profile of Lα in Figure 1.

In this paper we focus on the strong resonances (1–2) $P(5)$ and (4–3) $P(5)$ within 60 cm^{-1} of line center, as well as (0–2) $R(1)$, (0–2) $P(1)$, and (0–2) $R(2)$ in the far-red wing. The closest resonances (1–2) $R(6)$ and (3–3) $R(1)$ may be absent if Lα is self-reversed at line-center.

Lβ and higher lines in the H I (np–$1s$) series overlap the H_2 Lyman and Werner bands in $v'' = 0$ and $v'' = 1$. As discussed by Feldman and Fastie (1973), resonance fluorescence from Lβ can be important in regions where

TABLE 1

Lα–H_2 Resonance Fluorescent Lines

Lyman Line*	(v_l, J_l)†	T_{exc} (K)‡	$\Delta\nu$ (cm^{-1})§	f_l‖
(1–2) *P*(5)	(2, 5)	13,889	−27	2.91(−2)
(1–2) *R*(6)	(2, 6)	14,760	−3	3.45(−2)
(0–2) *R*(0)	(2, 0)	11,635	−104	4.42(−2)
(0–2) *R*(1)	(2, 1)	11,789	−134	2.95(−2)
(0–2) *R*(2)	(2, 2)	12,095	−231	2.65(−2)
(0–2) *P*(1)	(2, 1)	11,789	−249	1.47(−2)
(1–2) *R*(5)	(2, 5)	13,889	+362	3.49(−2)
(0–1) *R*(10)#	(1, 10)	14,243	+382	6.73(−3)
(0–1) *P*(10)#	(1, 10)	14,243	−313	6.12(−3)
(3–3) *R*(0)	(3, 0)	16,952	+45	3.53(−3)
(3–3) *R*(1)	(3, 1)	17,097	+9	2.35(−3)
(3–3) *P*(1)	(3, 1)	17,097	−94	1.18(−3)
(3–3) *R*(2)	(3, 2)	17,387	−93	2.12(−3)
(4–3) *P*(5)	(3, 5)	19,086	+60	9.32(−3)
(4–3) *R*(6)	(3, 6)	19,912	+46	1.10(−3)

* Spectroscopic notation: (1–2) *P*(5) denotes $v_u = 1$, $v_l = 2$; *P*-branch has $J_u = J_l - 1$; *R*-branch has $J_u = J_l + 1$.

† Lower level vibrational and rotation quantum numbers.

‡ Excitation temperature of lower level.

§ $(\nu - \nu_{L\alpha})$, where $\nu_{L\alpha} = 82{,}259.17\ cm^{-1}$.

‖ Absorption oscillator strength (Allison and Dalgarno 1970), with Hönl-London correction factor (Schadee 1967). Nonadiabatic corrections may be 10%–20%.

Energy levels and oscillator strengths uncertain because of nonadiabatic perturbations of upper levels (Julienne 1973; Ford 1975).

little neutral hydrogen is present. Upon encountering a column density $N(\mathrm{H\ I}) \geq (7 \times 10^{14}\ cm^{-2})(b/5\ km\ s^{-1})$, where b is the Doppler parameter, Lβ will be 90% converted to Lα. We therefore expect that in the cases of the solar emission lines or the interstellar medium, pumping from Lβ will be quite weak, unless the line is Doppler shifted out of the absorption profile.

The solar UV spectrum shows numerous other lines, which are 5%–25% as strong as Lα, but with much narrower profiles (FWHM ≈0.1 Å) (Cheng, Doschek, and Feldman 1976). Resonances with H_2 Lyman and Werner bands in $v'' = 0$ within 0.100 Å exist for N II (λ1084.562, λ1084.580), N III (λ989.790, 991.514, 991.579), and O VI (λ1031.945).

III. RESULTS

Because of the resonant nature of Lα excitation of H_2, the pumping rates and fluorescent line ratios depend both on the Lα emission profile and on Doppler shift. In the following discussion, we shall define our "standard model" to be an unshifted Lα Lorentz profile with 1 Å full width at half-maximum (FWHM) ($\Delta\nu_F = 67.7\ cm^{-1}$),

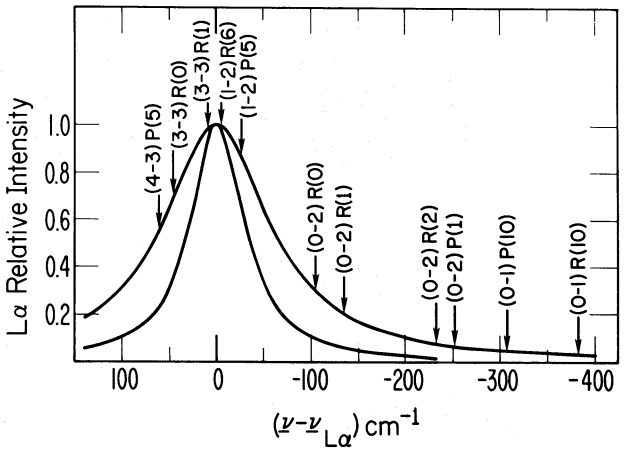

FIG. 1.—Location of H_2–Lα resonances, relative to Lα Lorentz emission profiles of 1 Å and 2 Å FWHM

in accordance with chromospheric observations (Basri *et al.* 1978). The photon number flux is then

$$\Phi(\nu) = \frac{2\Phi_0}{\pi\Delta\nu_F C}\,[1 + 4(\nu - \nu_{L\alpha})^2/(\Delta\nu_F)^2]^{-1}\ \mathrm{cm^{-2}\ s^{-1}\ Hz^{-1}}\,. \quad (1)$$

This model obviously represents only a zeroth-order approach to the problem. To model the sunspot emission accurately, one must follow the radiative transfer of Lα through the layers of H I between the Lα formation zone and the H_2, accounting for the effects of line broadening and core self-reversal. We hope to compute such models in the future.

The total resonant pumping rate of H_2 by Lα is given by the summation over lines,

$$P_{L\alpha} = n(H_2)\sum_i q(v_i, J_i)\sigma(v_i, J_i)\Phi(\nu_i)S_i(\tau_i)\ \mathrm{cm^{-3}\ s^{-1}}\,, \quad (2)$$

where $\Phi(\nu_i)$ is the number flux[1] at line (i), and where $q(v_i, J_i)$ and $\sigma(v_i, J_i)$ are, respectively, the H_2 fractional level populations and line-absorption cross sections. $S(\tau)$ is a line-saturation factor, described in more detail in Appendix A, which deals with optical depth effects.

We compute $q(v_i, J_i)$ for Boltzmann equilibrium, considering rotational states $J'' = 0$–15 in vibrational states $v'' = 0$–6. To model the solar emission lines, the H_2 density has been determined from the Saha equation (Mihalas 1970), with electrons provided by 16 metals of low ionization potential (Vernazza, Avrett, and Loeser 1973), and with dissociation constants for the various forms of hydrogen taken from Vardya (1961). The electron pressure $P_e = 10^{-2}$ dynes cm^{-2}, consistent with the value expected near solar temperature minimum (Vernazza *et al.*).

Figure 2 illustrates the H_2 density and the optically thin pumping cross sections for the strongest lines from $v'' = 2$ and $v'' = 3$ in our standard model. These effective cross sections are defined as $q(v_i, J_i)\sigma(v_i, J_i)\Phi(\nu_i)/\Phi_0$ (see eq. [1]). The peaks in the pumping near 2600 K result from the competition between the H_2 density (which falls with temperature) and the fractional level populations (which increase with temperature).

Differences between absorption from $v'' = 2$ and $v'' = 3$ and effects of Lα Doppler shift are shown in Figure 3. Although Lα should not be shifted in the solar chromosphere, one might expect shifts of up to 100 km s^{-1} in runaway stars or at different orbital phases of comets; much larger shifts are possible for Lα produced in the expanding envelopes of hot stars. The solid curves in Figure 3 represent optically thin pumping rates of (0–2) $R(1)$ and (4–3) $P(5)$ relative to the strongest resonance (1–2) $P(5)$; dashed lines represent relative rates for Lα redshifted (R) and blueshifted (B) by 100 km s^{-1}. The sense of these shifts may be understood by noting (Fig. 1) that (0–2) $R(1)$ and (1–2) $P(5)$ lie in the "red" wing of Lα, whereas (4–3) $P(5)$ lies in the "blue" wing. Hence Doppler shifts of Lα to the red or blue bring each of these lines on and off resonance. The fact that a blueshift of Lα increases (0–2) $R(1)$ relative to (1–2) $P(5)$ results from a differential effect: the former line lies farther into

[1] The H_2 absorption profile is assumed to be much narrower than the Lα emission profile.

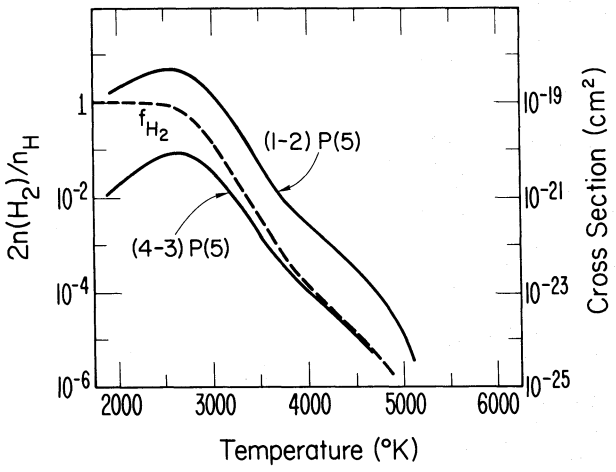

FIG. 2

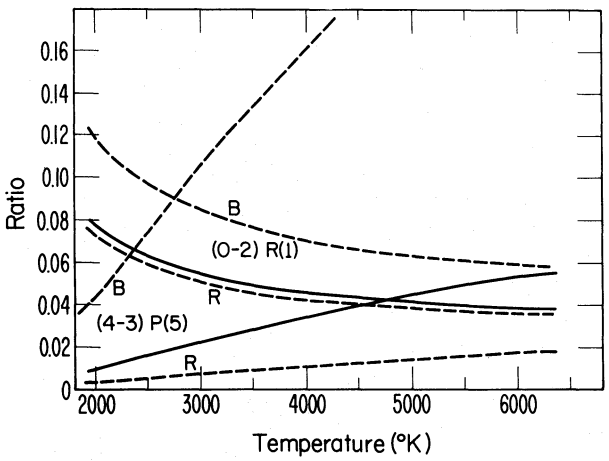

FIG. 3

FIG. 2.—Temperature dependences of Lα–H_2 resonant pumping cross sections and fractional H_2 density in LTE. Solid lines represent pumping cross sections for the strongest lines pumped from $v'' = 2$ and $v'' = 3$ defined as $q(v_i, J_i)\sigma(v_i, J_i)\Phi(\nu_i)/\Phi_0$ (see eq. [2] in text). Dashed line represents fractional H_2 density in Saha equilibrium, for electron pressure $P_e = 10^{-2}$ dynes cm^{-2}, appropriate near solar temperature minimum.

FIG. 3.—Temperature and Doppler shift dependences of the pumping ratios of (0–2) $R(1)$ and (4–3) $P(5)$, relative to (1–2) $P(5)$, for "standard model" (Lα FWHM = 67.7 cm^{-1}). Solid lines represent unshifted Lα; dashed lines represent Lα redshifted (R) and blueshifted (B) by 100 km s^{-1}.

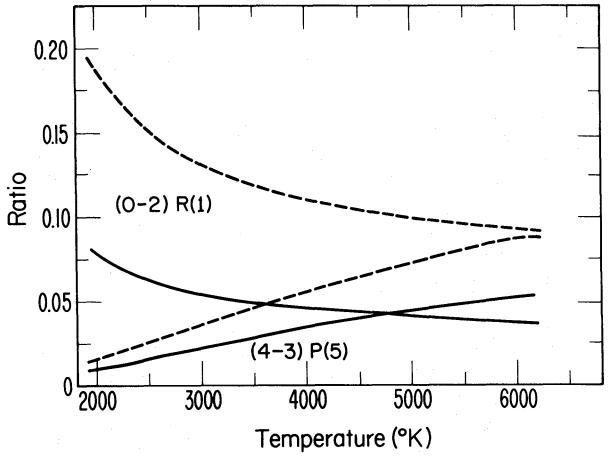

FIG. 4.—Temperature and Lα FWHM dependences of LTE pumping ratios in Fig. 2, relative to (1–2) $P(5)$. *Solid lines*, unshifted Lα with 1 Å FWHM (67.7 cm^{-1}); *dashed lines*, 2 Å FWHM.

the red wing and hence experiences a smaller relative decrease in intensity. The trends of these ratios with temperature reflect the changes in relative populations of levels in $v'' = 2$ and $v'' = 3$.

Figure 4 depicts the effect of changing the FWHM of the Lα profile. The solid lines show relative line ratios for the standard model (FWHM = 67.7 cm^{-1}), and dashed lines show ratios for FWHM = 135 cm^{-1}. The selected absorption lines lie in the wings of Lα (Fig. 1) and emphasize the sensitivity of pumping to the Lα line width. In an H II region or planetary nebula, the Lα profile will be much narrower (FWHM = 3 cm^{-1}, corresponding to 10 km s^{-1} thermal width). Resonant pumping of H_2 near these regions will most likely be limited to the lines (1–2) $R(6)$ and (3–3) $R(1)$. However, Wolf-Rayet and other emission-line stars exhibit strong, broad emission lines in the UV which would have noticeable effects on any nearby H_2.

IV. APPLICATIONS

a) Solar Emission Lines

We now apply our model to the H_2 solar emission lines observed by Jordan *et al.* (1977). The assumption of an idealized Lα emission profile allows us to infer resonance fluorescence rates which agree with the expectations of our simplified model. This represents the first step in a quantitative analysis of the process suggested by Jordan *et al.*, but detailed Lα transfer calculations in a realistic sunspot model will be required to assess the finer points.

As described in Appendix B, the H_2 ultraviolet observations determine the column densities $N^*(v', J')$ in levels of the excited electronic state. These data indicate that $N^*(1, 4) = (2.5 \pm 1) \times 10^4$ cm^{-2}, $N^*(0, 1) = (6 \pm 2) \times 10^4$ cm^{-2}, $N^*(0, 2) = (6 \times 10^3$ $cm^{-2})$, and $N^*(0, 9) = (6 \pm 4) \times 10^4$ cm^{-2}. Assuming a radiative lifetime $\tau^*(1, 4) = 5.74 \times 10^{-10}$ s (Allison and Dalgarno 1970), we find that an integrated Lα pumping of 4×10^{13} cm^{-2} s^{-1} is required in the line (1–2) $P(5)$. In similar fashion we derive pumping of roughly 10^{14} cm^{-2} s^{-1} and 10^{13} cm^{-2} s^{-1} in (0–2) $R(0)$ and (0–2) $R(1)$, respectively.

This integrated pumping may be related to the local pumping rate $P_{L\alpha}$ defined in equation (2), by replacing $n(H_2)q(v_i, J_i)$ with an effective column density $N_{H_2}(v_i, J_i)$. For an unshifted Lα profile with 1 Å FWHM, equation (2) indicates that the (1–2) $P(5)$ pumping requires $N_{H_2}(2, 5)\Phi_0 = 2.7 \times 10^{29}$ cm^{-4} s^{-1}. Taking $\Phi_0 = 1.4 \times 10^{16}$ cm^{-2} s^{-1}, the value at the solar surface, we see that $N_{H_2}(2, 5) \approx 2 \times 10^{13}$ cm^{-2}, corresponding to $N(H_2) \approx 5 \times 10^{15}$ cm^{-2} if a constant sunspot temperature of 3200 K is assumed. Within the uncertainties of profile shape at these depths the former column density is in reasonable agreement with the value expected for line saturation of (1–2) $P(5)$ ($f_i = 0.03$); see Appendix A.

The strong pumping in (0–2) $R(0)$ and (0–2) $R(1)$ suggests that there is substantial flux in the Lα wings ($\Delta\nu >$ 90 cm^{-1}) in the region where the H_2 is pumped. The chromospheric Lα illuminates the H_2 in this cool region only after traversing some depth in intermediate layers of atomic hydrogen. Consequently, the Lα emission profile in the H_2 zone will be broadened, and the wings will most likely depart from our assumed Lorentzian form. It is somewhat surprising that the H_2 emission is (apparently) limited to resonances within 200 cm^{-1} of line center. It will be interesting to compare the predictions of detailed Lα transfer calculations with observational limits on resonance fluorescence from lines in the far wings. Such calculations are also necessary to account in detail for the effects of variable temperature and line saturation.

The populating mechanism of ($v' = 0, J' = 9$) is unclear. Extrapolation from lines from lower rotational levels indicate that the H_2 Lyman lines (0–1) $P(10)$ and (0–1) $R(10)$ lie approximately 313 cm^{-1} and 382 cm^{-1} into the red and blue wings, respectively, of Lα. However, nonadiabatic perturbations of the B and C excited electronic states cause level shifts increasing as $J(J + 1)$ (Julienne 1973), and these wavelengths are uncertain.

Jordan *et al.* (1977) suggested that collisional processes from the nearby ($v' = 1, J' = 4$) level may be indicated, but this seems unlikely in view of the large A values from this state. Alternatively, the (0, 9) level may be excited by resonance fluorescence of C II λ1036.337 with the H_2 Lyman line (8–0) $R(8)$ at 1036.564 Å, or of N III λ991.579 with (12–0) $R(8)$. At this point, fluorescence by photons in the extreme wings of Lα seems the most likely explanation.

The apparent absence of lines pumped by (1–2) $R(6)$, the closest resonance, may reflect the self-reversal of Lα. The absence of fluorescence from (3–3) $R(1)$ probably results, as noted by Jordan *et al.*, from the self-reversal as well as lower population in $v'' = 3$. A careful search for fluorescence from key upper levels could determine the Lα profile and the temperature in the emission region. For example, limits on the fluorescence from (1–2) $R(5)$, (0–2) $P(1)$, and (0–2) $R(2)$, which lie in the extreme wings of Lα, combined with more precise measurements of the fluorescent intensities from (0–2) $R(0)$ and (0–2) $R(1)$ and detailed Lα transfer calculations, would improve our understanding of the trade-offs between H_2 abundance and Lα profile width at large depths. Once the profile is known, measurement (or upper limits) of the fluorescence from (0–2) $R(1)$ and (4–3) $P(5)$, relative to (1–2) $P(5)$, would provide a temperature diagnostic.

Lα has been observed to vary by 30% in time (Vidal-Madjar 1975) as well as spatially (Bruner *et al.* 1973). If the H_2 pumping lines are saturated, the sunspot fluorescence should show little response. The sensitivity of the molecular abundance to temperature should, however, restrict the fluorescence to the coolest regions.

The UV pumping of H_2 also produces infrared emission lines, as the molecules cascade through vibrational-rotational levels of the ground electronic state. Using the cascade-matrix formalism (Black and Dalgarno 1976), we find that 75%–80% of the molecules pumped by (1–2) $P(5)$ will pass through one of the $v'' = 1 \rightarrow 0$ quadrupole lines near 2 μm. Since the (1–2) $P(5)$ fluorescence returns to the ground electronic state in $R(3)$ and $P(5)$ lines, the IR fluorescence will be restricted to transitions between ortho- levels (odd-J), of which the $S(1)$, $S(3)$, $Q(1)$, and $Q(3)$ lines in the $v'' = 1 \rightarrow 0$ band will be the strongest. For typical photospheric densities and temperatures, however, collisions enforce LTE in the vibrational-rotational levels of the ground electronic state, and this fluorescence will be unobservable.

b) Interstellar Gas

Typical interstellar clouds are far too cool (Spitzer and Jenkins 1975) for vibrationally excited H_2 to exist in large amounts. However, 10–20 km s^{-1} shocks in molecular clouds, such as have been suggested to explain the Orion quadrupole emission lines (Gautier *et al.* 1976; Hollenbach and Shull 1977; Kwan 1977; London, McCray, and Chu 1977) would provide substantial excitation to $v'' = 2$ and $v'' = 3$. Vibrationally excited H_2 would also be produced by UV pumping from OB stars or planetary nebulae near molecular clouds (Black and Dalgarno 1976; Shull 1978; Beckwith, Persson, and Gatley 1978). If these regions are bathed in intense Lα, one would expect characteristic UV and IR fluorescence, as well as an absence of IR lines originating in levels pumped by Lα.

Since the Doppler width of Lα in an H II region or planetary is $\sim$10 km s^{-1} (3 cm^{-1}), only (1–2) $R(6)$ and (3–3) $R(1)$ are likely to be pumped. Expansion velocities of 10–25 km s^{-1} in these objects could introduce complexities, however. The Lα number flux at the edge of a Strömgren sphere of density n_e and radius R_s may be estimated as

$$\mathscr{F}_0 = \tfrac{1}{3} n_e^2 \alpha_H^{(2)} R_s \approx (9.5 \times 10^6 \text{ cm}^{-2} \text{ s}^{-1}) n_e^{4/3} N_{48}^{1/3} , \quad (3)$$

where $\alpha_H^{(2)}$ is the H recombination rate to excited levels (at 10^4 K), and where N_{48} is the stellar Lyman continuum flux in units 10^{48} s^{-1} (Panagia 1973). Absorption of Lα by dust within the H II region will diminish this somewhat. For a Gaussian Lα emission profile with Doppler width 3 cm^{-1}, the pumping rate of level ($v'' = 2, J'' = 6$) by the line (1–2) $R(6)$ is $(5.5 \times 10^{-8} \text{ s}^{-1}) n_e^{4/3} N_{48}^{1/3} \phi(\nu)$, where $\phi(\nu)$ is a line-overlap factor of order unity, accounting for the slight shift of the absorption profile. The radiative decay rate from (2, 6) is 1.5×10^{-6} s^{-1} (Turner, Kirby-Docken, and Dalgarno 1977), while the rotational collisional de-excitation rate at 4000 K is $\sim 10^{-10} n(H^0)$ s^{-1} (Nishimura 1968) or $\sim 10^{-11} n(H_2)$ s^{-1} (Green, Ramaswamy, and Rabitz 1978), depending on the relative densities of H^0 and H_2 in the cloud. Evidently, Lα fluorescence will deplete level (2, 6) before radiative decay for $n_e \geq 10$ cm^{-3}, while collisions are competitive with fluorescence for $n(H^0) \gtrsim 10^2 n_e^{4/3}$ or $n(H_2) \gtrsim 10^3 n_e^{4/3}$.

If Lα fluorescence is more rapid than radiative or collisional effects, one would expect the infrared $S(4)$, $Q(6)$, and $O(8)$ lines in the $v'' = 2 \rightarrow 0$ and $v'' = 2 \rightarrow 1$ bands to be absent. In view of atmospheric absorption, the most propitious lines to search would be (2–0) $S(4)$ (1.2545 μm), (2–1) $Q(6)$ (3.7249 μm), and (2–0) $O(8)$ (1.9662 μm). Beckwith *et al.* (1977) detected (2–1) $S(1)$ toward Orion at roughly 0.10 times the intensity of (1–0) $S(1)$; hence, meaningful upper limits on these weaker lines may require substantial integration.

The Lα fluorescence by (3–3) $R(1)$ will be much smaller, as a result of its lower oscillator strength. The effects on the IR emission from ($v'' = 3, J'' = 1$) will be nearly unobservable because of the small population $v'' = 3$.

c) Other Objects

A candidate object for the Lα–H_2 resonance fluorescence process must involve both strong Lα emission and vibrationally excited ($v'' \geq 2$) H_2. As suggested by Jordan *et al.* (1977), cool stars would be likely objects to show

emission similar to sunspots. Somewhat "closer to home," Jupiter and Saturn exhibit H_2 absorption bands in the IR, but it is doubtful whether their atmospheric temperatures are high enough to excite $v'' = 2$ ($T_{exc} = 12{,}000$ K). Comets would provide a very interesting laboratory to test the resonance fluorescence process, since one would expect Doppler shifts up to 100 km s^{-1} at various phases of the orbit. However, in addition to their cool temperatures, comets probably have most of their H in the form of ices.

Interstellar configurations involving a Wolf-Rayet or emission star near a dense cloud containing H_2 could produce observable effects on the UV pumping cascade of H_2. Since Lα and other emission lines in such stars are often 1500 km s^{-1} wide, many resonances with Lyman bands exist, including those from $v'' = 0$ in the cases of C II, N II, O VI, and other lines shortward of 1100 Å. One might then expect the populations of the high rotational levels of H_2 (Jura 1975) to show modifications observable with the *Copernicus* UV spectrometer. For example, *Copernicus* observations of the interstellar gas toward the WN5 star HD 50896 (Shull 1977) showed a dense ($n \approx 300$ cm^{-3}) cloud containing H_2 with a moderate rotational excitation temperature (~ 380 K). Although the distance of the cloud from the star is unknown (it must lie some minimum distance away as determined by the stages of ionization observed), the observations do serve to illustrate that configurations such as those described above may be possible.

I am grateful to T. Ayres, G. Basri, E. Chipman, H. Lamers, J. Linsky, R. London, R. McCray, and L. November for helpful discussions and to the referee for a number of suggestions. This work was supported by the National Science Foundation through grant AST 75-23590.

APPENDIX A

EFFECTS OF LINE SATURATION

In an optically thin situation, the integrated H_2–Lα resonant pumping in line (i) may be written (see eq. [2])

$$J_{L\alpha}^{(i)} = N(v_i, J_i)\sigma(v_i, J_i)\Phi(\nu_i) \text{ cm}^{-2} \text{ s}^{-1}, \tag{A1}$$

where $N(v_i, J_i)$ is the H_2 column density in the lower state. After a column density $N_c \approx (2.75 \times 10^{12} \text{ cm}^{-2}) \times f_i^{-1}(b/5 \text{ km s}^{-1})$ (assuming a Doppler parameter b and oscillator strength f_i), this line reaches optical depth unity at line center. If the Lα flux is constant with depth, the oscillator strength dependence in equation (A1) cancels, and the relative pumping ratios of various lines depend only on their flux-overlap factors $\Phi(\nu_i)$.

In the optically thick region ($1 \leq \tau_i \leq \tau_{max}$), the pumping rates must be multiplied by a shielding factor $S(\tau)$, which for lines on the Doppler portion of the curve of growth is given by (Shull 1978)

$$S_D(\tau) = \frac{(2)^{1/2}}{e} \frac{1}{\tau(\ln \tau)^{1/2}} . \tag{A2}$$

For constant Lα flux, this region contributes an additional pumping, roughly $(\ln \tau_{max})^{1/2}$ times the amount for $\tau_i = 1$; for $\tau_{max} = 10^2$–10^4, this represents a factor of only 2–3. At larger depths, the H_2 lines reach the damping portion of the curve of growth, where $S(\tau) \propto \tau^{-1/2}$. However, by this point the Lα will probably be scattered into the wings. For this reason, one might expect that the weaker lines from $v'' = 2$, or lines pumped from $v'' = 3$, would not reach their full saturated intensity.

APPENDIX B

The intensity I_{ij} of an emission line is related to the column density, N_i (cm^{-2}), in the upper level by

$$I_{ij} = \frac{N_i A_{ij}(\Delta E_{ij})}{4\pi} = (1.58 \times 10^{-9}) \frac{N_i A_{ij}}{\lambda_{ij} \text{ (Å)}} \text{ ergs cm}^{-2} \text{ s}^{-1} \text{ sr}^{-1}, \tag{B1}$$

where ΔE_{ij} is the transition energy and A_{ij} is the radiative transition rate. For the Lyman bands of H_2, the transition rate from ($vJ \rightarrow v''J''$) is

$$A(vJ, v''J'') = (6.67 \times 10^{15}) \left[\frac{g_l}{g_u} f_{lu} \lambda_{lu} \text{ (Å)}^{-2} \right] \text{ s}^{-1}, \tag{B2}$$

where

$$f_{lu} = f_{v'',v} \left(\frac{S_{J''}}{2J'' + 1} \right) \frac{\lambda_{v'',v}}{\lambda_{lu}} . \tag{B3}$$

Here g_l and g_u are statistical weights of the lower (v'', J'') and upper (vJ) levels, λ_{lu} is the transition wavelength, and

TABLE 2

H_2 SOLAR EMISSION LINES

Line	λ (Å)	A_{ij} (s^{-1})*	I_{ij}†	(v_i, J_i)‡	$N(v_i, J_i)$§
(1–3) $P(5)$.....	1271.93	3.92(8)	11	(1, 4)	2.3(4)
(1–3) $R(3)$.....	1257.80	3.21(8)	11	(1, 4)	2.7(4)
(1–4) $R(3)$.....	1314.62	5.97(7)	3	(1, 4)	4.2(4)
(1–5) $P(5)$.....	1387.35	5.29(7)	2	(1, 4)	3.3(4)
(1–6) $P(5)$.....	1446.13	4.01(8)	9.6	(1, 4)	2.2(4)
(1–6) $R(3)$.....	1431.01	3.28(8)	7.4	(1, 4)	2.0(4)
(1–7) $P(5)$.....	1504.79	5.90(8)	14	(1, 4)	2.3(4)
(1–7) $R(3)$.....	1489.57	4.81(8)	12	(1, 4)	2.3(4)
(1–8) $P(5)$.....	1562.41	3.94(8)	12	(1, 4)	3.0(4)
(1–8) $R(3)$.....	1547.35	3.21(8)	14	(1, 4)	4.3(4)
(0–4) $P(2)$.....	1338.57	1.03(8)	7.2	(0, 1)	5.9(4)
(0–4) $R(0)$.....	1333.48	5.17(7)	5.4	(0, 1)	8.8(4)
(0–6) $P(2)$.....	1460.17	5.26(7)	2.4	(0, 1)	4.2(4)
(0–6) $P(3)$.....	1463.83	4.28(8)	2.6	(0, 2)	5.7(3)
(0–6) $R(1)$.....	1454.97	2.86(8)	3.2	(0, 2)	1.0(4)
(0–4) $P(10)$.....	1393.45	7.47(7)	4.0	(0, 9)	4.7(4)
(0–4) $R(8)$.....	1363.58	7.02(7)	5.1	(0, 9)	6.3(4)
(0–5) $P(10)$.....	1453.02	6.46(7)	7.7	(0, 9)	1.1(5)
(0–5) $R(8)$.....	1422.55	6.06(7)	1.8	(0, 9)	2.7(4)

* Radiative transition rate.

† Observed line intensity (ergs cm^{-2} s^{-1} sr^{-1}) from Jordan *et al.* (1977).

‡ Upper state vibrational-rotational quantum numbers.

§ Column density in upper level inferred from data.

f_{lu} is the absorption oscillator strength, related to the band oscillator strength $f_{v'',v}$ (Allison and Dalgarno 1970) of the fictitious ($J = 0 \rightarrow J'' = 0$) transition of wavelength $\lambda_{v'',v}$ by the Hönl-London factor, $S_{J''}$. For the R-branch $S_{J''} = J'' + 1$; for the P-branch $S_{J''} = J''$.

Table 2 presents the A values for the observed sunspot lines, together with the inferred column densities in the upper level.

REFERENCES

Allison, A. C., and Dalgarno, A. 1970, *Atomic Data*, **1**, 289.
Basri, G., Linsky, J., Bartoe, J.-D. F., Brueckner, G., and VanHoosier, M. E. 1978, in preparation.
Beckwith, S., Becklin, E. E., Neugebauer, G., and Persson, S. E. 1977, *Bull. AAS*, **8**, 564.
Beckwith, S., Persson, S. E., and Gatley, I. 1978, *Ap. J. (Letters)*, **219**, L33.
Black, J. H., and Dalgarno, A. 1976, *Ap. J.*, **203**, 132.
Bruner, E. C., Parker, R. W., Chipman, E., and Stephens, R. 1973, *Ap. J. (Letters)*, **182**, L33.
Carruthers, G. B. 1970, *Ap. J. (Letters)*, **161**, L81.
Cheng, C.-C., Doschek, G. A., and Feldman, U. 1976, *Ap. J.*, **210**, 836.
Cochran, W. D., Gelfand, J., and Smith, W. H. 1976, *Ap. J.*, **207**, 639.
Feldman, P. D., and Fastie, W. G. 1973, *Ap. J. (Letters)*, **185**, L101.
Fink, U., Wiggins, T., and Rank, D. 1965, *J. Molec. Spectrosc.*, **18**, 384.
Ford, A. L. 1975, *J. Molec. Spectrosc.*, **56**, 251.
Gautier, N., Fink, U., Treffers, R. R., and Larson, H. P. 1976, *Ap. J. (Letters)*, **207**, L129.
Grasdalen, G., and Joyce, R. R. 1976, *Bull. AAS*, **8**, 349.
Green, S., Ramaswamy, R., and Rabitz, H. 1978, *Ap. J. Suppl.*, **36**, 483.
Herzberg, G. 1950, *Spectra of Diatomic Molecules* (Princeton: Van Nostrand).
Herzberg, G., and Howe, L. L. 1959, *Canadian J. Phys.*, **37**, 636.
Hollenbach, D. J., and Shull, J. M. 1977, *Ap. J.*, **216**, 419.
Jordan, C., Brueckner, G. E., Bartoe, J.-D. F., Sandlin, G. D., and VanHoosier, M. E. 1977, *Nature*, **270**, 326.
Julienne, P. S. 1973, *J. Molec. Spectrosc.*, **48**, 508.
Jura, M. 1975, *Ap. J.*, **197**, 581.
Kwan, J. 1977, *Ap. J.*, **216**, 713.
London, R., McCray, R., and Chu, S.-I. 1977, *Ap. J.*, **217**, 442.
Mihalas, D. 1970, *Stellar Atmospheres* (San Francisco: Freeman).
Morton, D. C., and Dinerstein, H. L. 1976, *Ap. J.*, **204**, 1.
Nishimura, S. 1968, *Ann. Tokyo Astr. Obs.*, Ser. 2, **11**, 33.
Panagia, N. 1973, *A.J.*, **78**, 929.
Schadee, A. 1967, *J. Quant. Spectrosc. Rad. Transf.*, **7**, 169.
Shull, J. M. 1977, *Ap. J.*, **212**, 102.
———. 1978, *Ap. J.*, **219**, 877.
Spitzer, L., Drake, J. F., Jenkins, E. B., Morton, D. C., Rogerson, J. B., and York, D. G. 1973, *Ap. J. (Letters)*, **181**, L116.
Spitzer, L., and Jenkins, E. B. 1975, *Ann. Rev. Astr. Ap.*, **13**, 133.
Stephens, T. L., and Dalgarno, A. 1970, *J. Quant. Spectrosc. Rad. Transf.*, **12**, 569.
Treffers, R. R., Fink, U., Larson, H. P., and Gautier, T. N. 1976, *Ap. J.*, **209**, 793.
Turner, J., Kirby-Docken, K., and Dalgarno, A. 1977, *Ap. J. Suppl.*, **35**, 281.
Vardya, M. S. 1961, *Ap. J.*, **133**, 107.
Vernazza, J. E., Avrett, E. H., and Loeser, R. 1973, *Ap. J.*, **184**, 605.
Vidal-Madjar, A. 1975, *Solar Phys.*, **40**, 69.

J. MICHAEL SHULL: Joint Institute for Laboratory Astrophysics, University of Colorado, Boulder, CO 80309